Molecular Crystals and Liquid Crystals Incorporating Nonlinear Optics

Publication details, including instructions for authors and subscription information:
http://www.tandfonline.com/loi/gmcl17

Resonant Nonlinear Optical Processes and Charge Carrier Dynamics in Photoresponsive Polymers

P. N. Prasad [a] , J. Swiatkiewicz [a] & J. Pfleger [a]

[a] Department of Chemistry, State University of New York at Buffalo, Buffalo, New York, 14214

Version of record first published: 28 Mar 2007.

To cite this article: P. N. Prasad , J. Swiatkiewicz & J. Pfleger (1988): Resonant Nonlinear Optical Processes and Charge Carrier Dynamics in Photoresponsive Polymers, Molecular Crystals and Liquid Crystals Incorporating Nonlinear Optics, 160:1, 53-68

To link to this article: http://dx.doi.org/10.1080/15421408808083000

Mol. Cryst. Liq. Cryst., 1988, Vol. 160, pp. 53–68
Reprints available directly from the publisher
Photocopying permitted by license only

Printed in the United States of America

Resonant Nonlinear Optical Processes and Charge Carrier Dynamics in Photoresponsive Polymers

P. N. PRASAD, J. SWIATKIEWICZ and J. PFLEGER

Department of Chemistry, State University of New York at Buffalo, Buffalo, New York 14214

Resonant third order optical nonlinearity, $\chi^{(3)}$, in several photoresponsive polymers is studied by picosecond and femtosecond degenerate four wave mixing to investigate the role of photoexcited charge carriers. Both the magnitude and the response time of the observed optical nonlinearities seem to vary over a wide range. In the case of the poly-*N*-vinyl carbazole:trinitrofluorenone polymer composite photoconductor, the observed resonant $\chi^{(3)}$, dependent on the composition of the composite, is attributed to the photoexcited correlated electron-hole pairs with a response time (decay time) in hundreds of picoseconds. In the case of a soluble polyacetylene-polymethyl methacrylate graft co-polymer, the observed resonant $\chi^{(3)}$ has an extremely fast initial decay and is consistent with what can be expected from the intrachain soliton dynamics. In the case of an electrochemically formed polymer, specifically polythiophene, we observe a relatively large $\chi^{(3)}$ with, again, a very fast initial decay in subpicoseconds consistent with the intrachain polaronic processes. An in situ study of the nonlinear optical behavior as a function electrochemical redox cycle shows a drastic reduction of the overall $\chi^{(3)}$ as the film is oxidized.

INTRODUCTION

The science and technology of light-wave devices have received international attention because of their importance in optical information storage, optical signal processing and optical computing. Nonlinear optical phenomena are of significant importance in relation to the light-wave devices because they can be used to design optical switches, optical logics, spatial light modulators and harmonic generators for optical processing of information. The potential speed

(subpicoseconds) and large bandwidth capability of optical devices, and their capability for parallel processing of information makes optical signal processing and optical computers very attractive.

The nonlinear optical effects involve simultaneous interaction of more than one photon with a system whereby a coherent response in the form of another photon is generated at a phase-matched angle. In the dipolar approximation, the induced dipole, $\Delta\mu$, in an atom or a molecule by an external field E (due to radiation can be written as[1]

$$\Delta\mu = \alpha \cdot E + \beta : E\,E + \gamma \vdots E\,E\,E + \ldots, \tag{1}$$

where the vector quantities μ and E are related by the tensor quantities α, β, and γ which are known as polarizability, hyperpolarizability and second hyperpolarizability. The polarization terms involving β and γ give rise to second order and third order nonlinear optical effects, respectively.

The corresponding polarizations induced in a macroscopic or bulk medium (consisting of ensembles of atoms or molecules) can similarly be expressed in terms of bulk susceptibilities as

$$P = \chi^{(1)}E + \chi^{(2)} : E\,E + \chi^{(3)} \vdots E\,E\,E + \ldots \tag{2}$$

In this equation the second and third-order optical susceptibilities, $\chi^{(2)}$ and $\chi^{(3)}$, describe the nonlinear behavior. The term $\chi^{(2)}$ is responsible for second order effects such as electro-optic effects and second harmonic generation. It can, in a simple model, be related to β by orientational averaging β over molecules in a molecular assembly and correcting for local field. It has a non-vanishing value only in an aligned non-centrosymmetric medium. The third-order nonlinear optical susceptibility, $\chi^{(3)}$, gives rise to a rich variety of effects, such as third-harmonic generation and nonlinear refractive index (intensity dependent)

$$n = n_0 + n_2 I \quad \text{where} \quad n_2 \propto \chi^{(3)}. \tag{3}$$

Another manifestation of $\chi^{(3)}$ is optical phase conjugation in degenerate four wave mixing (DFWM).[2] In this process three input beams $I_1(\omega)$, $I_2(\omega)$, and $I_3(\omega)$ (all with the same frequency ω, hence degenerate) interact in the medium in the geometry where $I_1(\omega)$ and $I_2(\omega)$ counterpropagate and $I_3(\omega)$, the probe beam, is incident at a small angle θ. The third-order optical nonlinearity of the medium

generates a coherent beam $I_4(\omega)$ which, in this geometry, counter-propagates to $I_3(\omega)$ or, in other words, is the phase conjugate of $I_3(\omega)$. The intensity $I_4(\omega)$ is given as

$$I_4(\omega) \alpha I_1(\omega)I_2(\omega)I_3(\omega) \frac{\{\chi^{(3)}\}^2}{n_0^4}. \quad (4)$$

Therefore, DFWM experiments also provide a method of studying $\chi^{(3)}$.

The degenerate four wave mixing process can be visualized as follows[3]: the beams $I_1(\omega)$ and $I_3(\omega)$ incident at an angle θ form a transient diffraction grating which diffracts the beam $I_2(\omega)$ into $I_4(\omega)$. For $\chi^{(3)}$ measurements, we are interested only in the grating formed due to electronic nonlinearity and not the grating formed by other processes such as thermal effects

For weak intermolecular coupling, one uses an oriented gas model and relates the microscopic nonlinearity γ with the bulk nonlinearity $\chi^{(3)}$ using the Lorentz approximation for the local field correction. In such a case

$$\chi^{(3)}(-\omega_4; \omega_1, \omega_2, \omega_3) = F(\omega_1)F(\omega_2)F(\omega_3)F(\omega_4) \sum_n \langle \gamma^n(\theta, \phi)\rangle \quad (5)$$

In this equation $F(\omega_1)$ represents the local field of frequency ω_1. The summation n runs over all molecular sites to give orientational averaging of $\langle\gamma\rangle$. The two limits are (i) all polymer chains aligned in the same direction in which case $\Sigma_n\langle\gamma^n(\theta, \phi)\rangle = N\gamma_{zzzz}$ and (ii) a completely amorphous polymer for which $\Sigma_n\langle\gamma^n(\theta, \phi)\rangle = 1/5\, N\gamma_{zzzz}$. The term N represents the number density. In either case, a large value of γ produces a large $\chi^{(3)}$. In this model, therefore, the optical nonlinearity of a material is determined by its microscopic nonlinearity γ.

The second-order effect in organic system, has been the subject of relatively more attention in the past and its understanding is more mature.[4–6] Theoretical recipes have been formulated to molecularly engineer structures which can be expected to show enhanced second order optical nonlinearity. In comparison, the origin of third order effects in organics is not well understood. A simple one dimensional pseudopotential model has been used to explain the large π-electron contribution to $\chi^{(3)}$ for conjugated polymeric systems.[7] In this model, the second hyperpolarizability γ for a conjugated polymer is largest along the polymer chain direction (z) and is related to the inverse

sixth power of the bandgap. The larger is the effective π-electron conjugation, the smaller is the bandgap resulting in an increased value for γ_{zzzz}.

The $\chi^{(3)}$ processes are expected to play an important role in optical devices. The concept of optical switches and optical bistable devices to be utilized in optical computing and optical communications is based on the property of intensity dependent refractive index. The concept of optical phase conjugation important for dynamic holography utilizes degenerate four wave mixing. Polymers containing π-electron conjugated structures have shown promises as third-order nonlinear optical materials since the largest nonresonant optical nonlinearity and fastest (femtosecond) response time have been observed for such polymers. Polymeric structures also offer the flexibility to modify the chemical structure, conformation, and shape. Therefore, their properties can be tailored to suit a specific application.

For this reason, efforts in the past have been focused on conjugated polymeric structures which have large γ derived from π-electron contribution.[6] This ad hoc approach based only on π-conjugation, however, has stifled the progress because the largest nonresonant $\chi^{(3)}$ observed so far in conjugated structures has only been $<10^{-9}$ esu. This value is not large enough for any practical devices which would like to use only small switching energy. One, therefore, has to find ways, other than conjugation alone, to enhance optical nonlinearity.

The role of charge-carriers in determining optical nonlinearities in inorganic semiconductors and photoconductors has been widely investigated. There has been a great deal of interest recently in multiple quantum well semiconductors.[7] Because of the two dimensional confinement of the photogenerated charge carriers in potential wells, the multiple quantum well systems exhibit greatly enhanced effective $\chi^{(3)}$. A corresponding evaluation of optical nonlinearities derived from charge carriers in organic semiconductors and photoconductors is lacking.

Organic polymeric systems exhibit a rich variety of charge-carrier dynamics and novel types of excitations.[8] In organic crystals and polymers, in general, coulomb bound electron-hole pairs are formed after photoexcitation. These pairs can undergo geminate recombination. Alternatively, they can undergo electric field assisted Onsager dissociation to form free carriers. In conjugated polymeric structures with bond alternation, the inherent coupling of electronic excitations with chain distortions produce novel excitations such as charged solitons, polarons and bipolarons. These charge carriers can either be generated by chemical doping or by photoexcitation. In the latter

type systems, the photoinduced generation of solitons and polarons leads to formation of mid gap states by dynamic distortion which also produce a considerable redistribution of oscillator strength.[9] Such a shift of oscillator strength provides a mechanism for resonant optical nonlinearity.

Therefore, the study of the optical nonlinearity in photoresponsive polymers where various charge carriers can be photoinduced is of great importance. However, very few studies of optical nonlinearity in photoresponsive system have been conducted. In this paper we present results from picosecond and subpicosecond degenerate four wave mixing studies of several photoresponsive polymers to examine the nature of resonant optical nonlinearity derived from the photogeneration of charge carriers. Specifically, three different types of systems will be discussed. These are: (i) poly-*N*-vinyl carbazole: trinitrofluorenone (PVK:TNF) polymer composite photoconductor; (ii) polyacetylene in the soluble form of a polyacetylene-polymethylmethacrylate (PA:PMMA) graft copolymer; and (iii) polythiophene in the reduced (undoped) and oxidized forms. In the case of the PVK:TNF system, we have investigated the role of photoinduced electron-hole pairs in determining the optical nonlinearity and its time response. In the case of PA:PMMA we examined the solitonic contribution to optical nonlinearity. For polythiophene we have conducted an in-situ electrochemical study of $\chi^{(3)}$ as a function of the redox cycle.

EXPERIMENTAL

1. Degenerate four wave mixing:

Degenerate four wave mixing (DFWM) provides a convenient method of measuring $\chi^{(3)}$. In a backward wave geometry for DFWM two beams I_1 and I_2 are counterpropagating and a third beam, I_3, is incident at a small angle; the signal, I_4, is the phase conjugate of I_3. In this arrangement the phase-matching requirement is automatically satisfied. Since all the input optical frequencies and the output optical frequency are of the same value, one measures $\chi^{(3)}(-\omega; \omega, \omega, \omega)$. This $\chi^{(3)}$ value is an important parameter for the design of devices utilizing optical switching and bistability. Furthermore, as we have demonstrated[10,11] from the measurements conducted in our laboratory, one can conveniently measure the anisotropy and time-response of $\chi^{(3)}$. Since thermal effects and excited state gratings also contribute to the degenerate four wave mixing signal, the capability to go to

time resolution of picoseconds and femtoseconds is needed to separate the various contributions. In our laboratory, we have two arrangements which can be used for this purpose. In the first arrangement, a CW mode-locked and Q-switched Nd-Yag laser is used to synchronously pump a dye laser which is subsequently cavity-dumped. The resulting pulses from the dye laser are about ~10μJ in energy and ~40ps wide. The repetition rate is 50–500Hz. The system, therefore, provides a medium peak power, high repetition rate picosecond pulses. This experimental arrangement also incorporates a long delay line of 18ns which is needed to observe the thermal effects. This arrangement is used to characterize and investigate any thermal effects present at a given wavelength. The thermal effect generates ultrasonic phonons and the acoustic ringing can be seen over tens of nanoseconds. The second arrangement provides a time-resolution of ~350 femtoseconds and very high peak power. This system schematically represented by Figure 1 consists of a CW mode-locked Nd-Yag laser, the pulses from which are compressed in a fiber-optics pulse compressor, and subsequently frequency doubled. The frequency doubled output is stabilized by a stabilizer unit, and then used to sync-pump a dye laser. The dye pulses are subsequently amplified

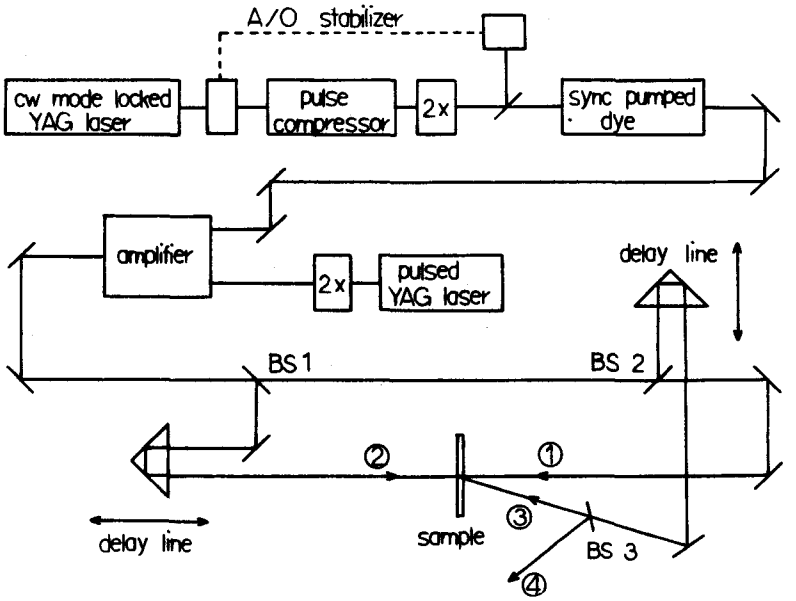

FIGURE 1 Schematics of our laser system for femtosecond degenerate four wave mixing studies. A/O = acousto optic; BS = beam splitters.

in a PDA amplifier (from Spectra-Physics) which is pumped by a Quanta-Ray model DCR-2A pulse Nd-Yag laser. The resulting pulses are ~350 femtoseconds wide with a pulse energy of 0.5mJ and at a repetition rate of 30Hz. This system was used on samples where we needed ultimate time-resolutions of femtoseconds to distinguish between resonant and non-resonant $\chi^{(3)}$ processes. The effective $\chi^{(3)}$ values of all the samples were obtained using CS_2 as the reference material. This method has been described in earlier publications.[10,11]

2. Film preparation and characterization:

A standard PVK sample of typical mol. wt. ~830000 obtained from Aldrich was used without further purification. TNF, also obtained from Aldrich, was purified by repeated crystallization from a tetrahydrofuran (THF) solution. Samples of various PVK:TNF compositions (e.g., 2:1, 4:1, 8:1, 16:1 and 32:1) were prepared by first dissolving completely the desired molar ratios of the components in THF and then coating the viscous solution on glass substrates by the doctor-blading technique. Thin sample films (3–6 μm) thus prepared were then dried at room temperature. To characterize these films, the linear absorption coefficient (for absorption loss correction), the linear refractive index and the sample thickness were measured. A method proposed by Ding and Garmire[12] which utilizes the m-lines of a quasi-wave guide was used to determine the refractive index of the films. The quasi-wave guide was formed by depositing the polymer film on the base of a prism. The refractive index of the samples was found to be ~1.330 at 602 nm. The wavelength of 602 nm used for the DFWM experiment provides excitation into the charge transfer band of the PVK:TNF system.

The details of preparation of the polyacetylene-polymethylmethacrylate graft co-polymer are described elsewhere.[13] The powder form of polyacetylene was first formed by using a Ziegler-Natta catalyst. Then the polymethylmethacrylate was grafted on it by using Na^+ doped polyacetylene as the initiator for anionic polymerization. Thin films of the co-polymer were cast on a glass slide by using a toluene solution for spin coating. The absorption spectrum of the film shows that the absorption maximum is shifted to shorter wavelength as compared to the typical Shirakawa polyacetylene indicating that the effective conjugation length in the PA/PMMA graft copolymer is shorter. From the absolute value of absorption coefficient, the molar ratio of [MMA]: [-CH-] was estimated to be 10^2.

Approximately a 1 μm thick film of polythiophene was prepared

by electrochemical oxidation of a 10^{-2}M solution of 2,2'-bithiophene in acetonitrile with tetrabutyl ammonium tetrafluoroborate as the supporting electrolyte at 0.1M concentration. Details of this procedure exist in the literature.[14] A typical three electrode electrochemical cell was used in which the working electrode was a In_2O_3-SnO_2 coated transparent glass electrode. For in-situ optical and electrochemical studies, a standard 1 cm optical cuvette was used. An EG&G PARC model 175 programmer in conjugation with a 173 potentiostat was used to carry out the electrochemical experiments.

RESULTS AND DISCUSSIONS

a) Poly-*N*-vinyl carbazole: Trinitrofluorenone polymer composite:

The degenerate four wave mixing (DFWM) signal intensity obtained as a function of the backward beam delay was investigated for polymer composites with different PVK:TNF compositions (2:1, 4:1, 8:1, 16:1 and 32:1). In Figure 2, time-resolved DFWM signals for two different compositions (2:1 and 16:1) are displayed. In each case, we observed a sharp rise of the zero-time signal which then decays by hundreds of picoseconds. The decay of the zero time signal is superimposed on an ultrasonic modulation which results from density excursion due to local heating by nonradiative relaxations. A comparison of the time-resolved DFWM signal behavior reveals the following characteristics as the concentration of TNF is decreased:

(i) The strength of the zero-time signal decreases
(ii) The decay of the zero-time signal becomes slower
(iii) The ultrasonic modulation becomes weaker

The excitation wavelength of 602 nm falls within the charge-transfer band of the PVK:TNF system. To understand the DFWM process under resonant conditions, the picture of a laser induced dynamic grating is very useful. In this model, two beams I_1 and I_3 cross at an angle θ in the material to form an intensity grating which results in a corresponding material excitation grating. A time-delayed beam I_2 is diffracted from this grating to produce output beam I_4. The grating efficiency η described as I_4/I_3 is given as[3]

$$\eta^{\lambda} \alpha \left(\frac{\partial n}{\partial x}\right)^2 g(\lambda)^2 I^{2\beta}(\lambda) f^2(t, \theta)$$

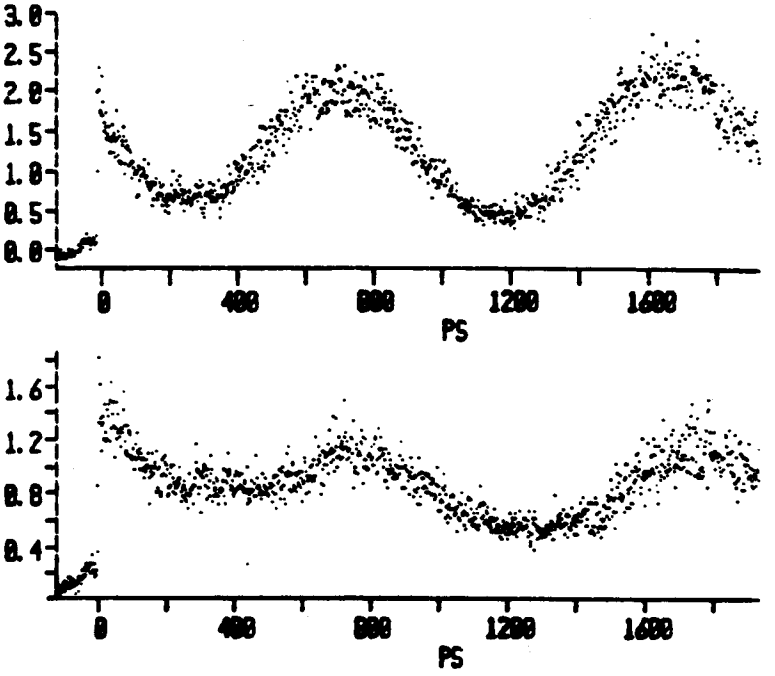

FIGURE 2 The observed time-resolved degenerate four wave mixing signal (in arbitrary units) is plotted as a function of the backward beam time delay for the PVK:TNF samples of two different compositions: 2:1(top) and 16:1(bottom).

Here x relates to the excitation density and $g(\lambda)$ is the quantum yield at wavelength λ. The term f is a function of crossing angle θ and time delay between the I_2 beam and the beams I_1 and I_3. The exponent β depends on the nature of the photon process.

In the case of PVK:TNF system, the intensity dependence of the DFWM signal yields $\beta = 1$. In other words, the grating is created by a one-photon resonance leading to the excitation of the charge-transfer band. Figure 3 provides a schematics of the photophysics of the PVK:TNF system following excitation into the charge transfer band.[15] The appearance of the ultrasonic modulation is caused by local heating due to nonradiative relaxations. The observation that the zero-time signal intensity is dependent on the concentration of TNF, and, consequently, on the concentration of the charge-transfer centers supports the hypothesis that the observed third order nonlinearity is derived from the thermalized correlated charge-pairs (excitons). We also attempted to use electric field effect to examine the effect on Onsager dissociation and hence the role of free carriers in

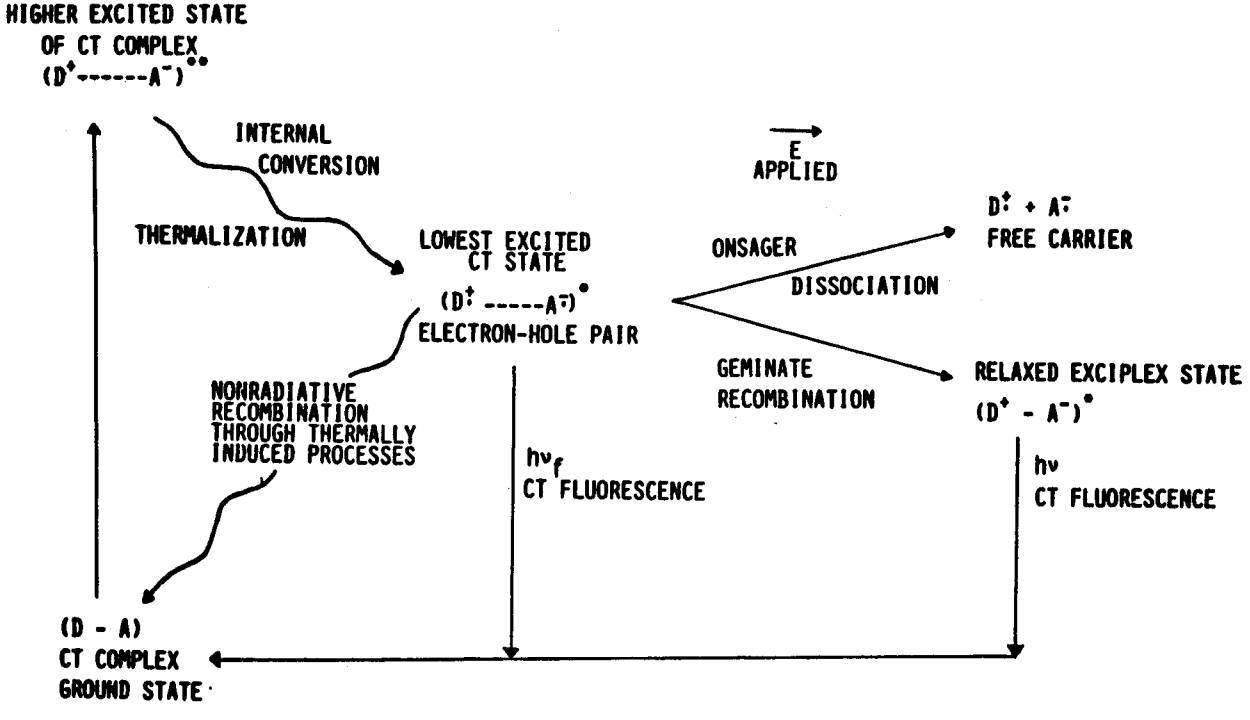

FIGURE 3 Schematics of various photophysical processes in the PVK:TNF system following excitation into the charge transfer band.

determining the $\chi^{(3)}$ behavior. We could only use a DC field of 3×10^4 V/cm before the breakdown occurred. No significant effect on the signal was observed. From these studies we conclude that the third order nonlinearity in the PVK:TNF photoconductor under charge-transfer excitation is dominated by the contribution due to correlated electron-hole pairs. A progressive increase of the zero-time decay time with a decrease in the TNF concentration can be explained by assuming that the decay component derived from the migration of excitons is reduced when the TNF concentration (hence the concentration of the charge transfer center) is decreased. An analysis using a diffusion model yielded the diffusion constant to be equal to 10^{-4} cm^2s^{-1}. The magnitude of the effective $\chi^{(3)}$ obtained for the PVK:TNF sample of composition 2:1 was found to be 2.3×10^{-11} esu. Therefore, the resonant processes in the PVK:TNF photoconductor does not provide a large $\chi^{(3)}$ and also has the disadvantage of a much longer decay time and ultrasonic modulation, the latter lasting up to tens of nanoseconds. The ultrasonic modulation can be a serious problem in resonant process in organics which often involve non-radiative relaxation. This will imply that even though the switch-on time may be very fast, one has to wait for a long time for a complete recovery before the process can be switched on again.

b) Polyacetylene-polymethylmethacrylate graft co-polymer:

The 602 nm excitation falls within the absorption band of polyacetylene (PA) in the PA-PMMA graft co-polymer form. The degenerate four wave mixing signal for the PA-PMMA graft copolymer obtained as a function of the backward beam time delay is shown in Figure 4. In contrast to the PVK:TNF system, the DFWM signal obtained from the PA-PMMA system decays extremely fast (within picoseconds) and under low intensities (far from saturation) shows no significant ultrasonic modulation. In other words, the intensity of the signal derived from ultrasonic modulation is considerably weaker than the zero-time signal. The magnitude of $\chi^{(3)}$ when scaled with the composition of the PA, yields a value of $\sim 10^{-10}$ esu for polyacetylene. This value is in close agreement with that reported for pure polyacetylene by using third-harmonic generation.[16,17] The higher value obtained for pure polyacetylene can be attributed to the higher conjugation length (smaller band gap) for pure polyacetylene compared with that for the PA-PMMA co-polymer. This result indicates that mainly the intrachain dynamics in polyacetylene contributes to $\chi^{(3)}$. A temperature dependence study indicates that the magnitude of $\chi^{(3)}$

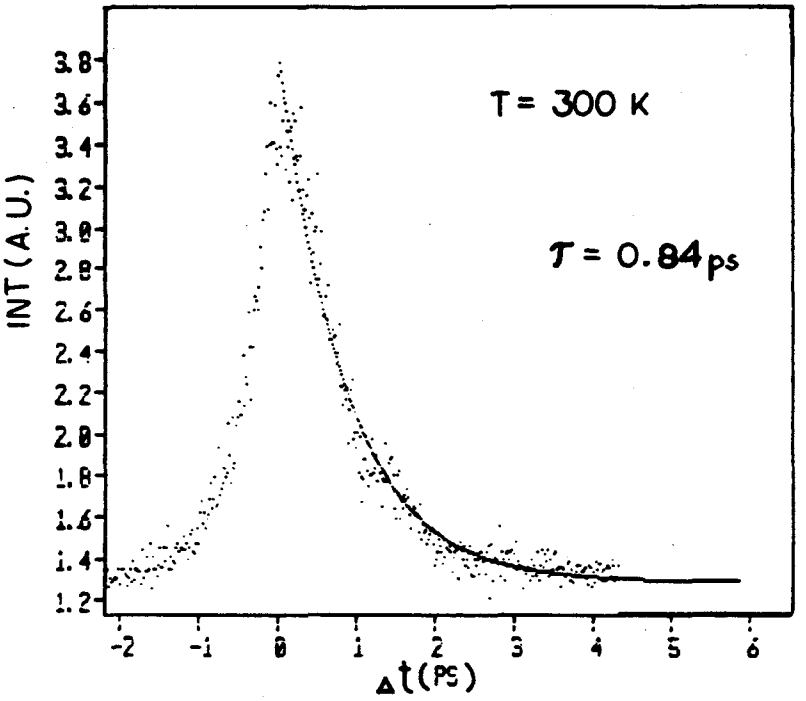

FIGURE 4 The degenerate four wave mixing signal obtained for the PA-PMMA graft copolymer is plotted as a function of the backward beam time delay.

or its time-response does not change significantly in going from room temperature to liquid nitrogen.

The theoretical work of Su and Schrieffer[18] proposes that the photoexcitation across the bandgap in polyacetylene would lead to a rapid chain distortion because of the coupling of the π-electron with the conformational distortion and would produce a soliton-antisoliton pair. The femtosecond time-resolved studies have shown that such distortions occur within femtoseconds to produce new states whereby a redistribution of oscillator strength occurs to lead to photoinduced absorption at new frequencies (midgap states) or photoinduced bleaching at the excitation frequency.[19,20] This change in absorbance, $\Delta\alpha$, decays initially very fast due to recombination of the soliton-antisoliton pairs. In the model where the absorbance change $\Delta\alpha$ due to photogeneration of the soliton-antisoliton pair produces a change of the complex refractive index, $\Delta\tilde{n}$, which in turn contributes to $\chi^{(3)}$, the temporal response of $\chi^{(3)}$ would be determined by that of $\Delta\alpha$. The observed time decay behavior of $\chi^{(3)}$ is consistent with this mech-

anism. Again, a similarity in the temporal behavior of $\chi^{(3)}$ observed in the PA-PMMA composite and that of $\Delta\alpha$ reported for pure polyacetylene, lends support to the suggestion that mainly intrachain dynamics contribute to the nonlinear processes in polyacetylenes.[16]

c) Polythiophene:

Polythiophene bond alternation yields a nondegenerate ground state. Therefore, the charge carriers coupled with the conformational deformation produce excitations such as polarons and bipolarons. Again, transient photoexcitation studies provide evidence for the formation of polarons and, subsequently, bipolarons.[21] The time-resolved DFWM signal obtained for polythiophene with ~350fs pulses is shown in Figure 5. A sharp rise in the signal is observed, the rise time being limited by the resolution of our optical pulses. The decay is broader than the pulse autocorrelation. The initial decay is fast with a decay time of about 1 picosecond followed by a slower nonexponential decay. The behavior again is similar to that reported for the transient absorption, $\Delta\alpha$, observed for polyacetylene; it is consistent with the mechanism of photoinduced conformation deformation and, consequently, redistribution of oscillator strength to new states in the gap as a mechanism for optical nonlinearity. The magnitude of $\chi^{(3)}$ calculated from the DFWM signal is $\sim 4 \times 10^{-10}$ esu. Within the conditions of the experiment, no detectable ultrasonic modulation is observed.

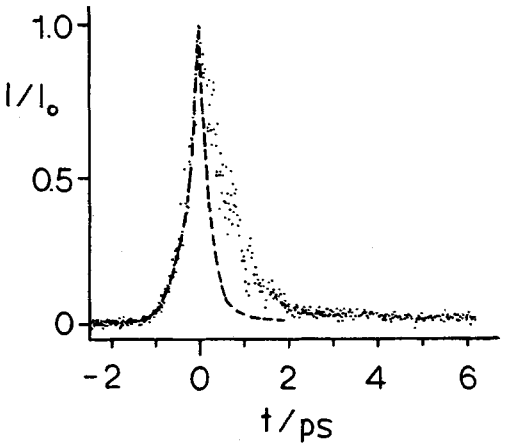

FIGURE 5 Femtosecond time-resolved degenerate four-wave mixing signal for polythiophene is displayed by the dotted curve. The dashed curve represented the autocorrelation of the laser pulses.

To examine the effect of chemical doping, we conducted the DFWM experiment as a function of electrochemical redox cycle. This result is shown in Figure 6. This study reveals a dramatic effect when the polymer is oxidized with a charge of only 3% to that used for the polymerization of the sample. This is the level of electrochemical doping at which polaron concentration (and hence spin) is maximum.[22,25] The linear absorption changes only slightly, but $\chi^{(3)}$ (corrected for linear absorption) reduces drastically. Past this level of electrochemical doping, the DFWM signal is almost within the noise level and remains at this level through further oxidation up to the maximum of electrochemical doping. Now going again through the reduction cycle, the original $\chi^{(3)}$ value is finally restored. The observed decrease of the overall $\chi^{(3)}$ during the electrochemical oxidation cycle can have two possible explanations: (i) the resonance contribution derived from $\Delta\alpha$ is changing due to a change of $\Delta\alpha$ during the doping process and (ii) the second hyperpolarizability and, hence, $\chi^{(3)}$ derived from the π-electron conjugation changes due to a change in π-electron correlation by the electrochemical oxidation. Silbey and co-workers[24] have shown that the introduction of polaronic defects leads to an increase in the non-resonant $\chi^{(3)}$ derived from the π-electron conjugation. Also, there is a change in the sign of $\chi^{(3)}$. Since at this time we do not know the frequency dispersion of $\chi^{(3)}$, it is difficult to provide a definite explanation for the observed effect. In order to understand the mechanism of the observed reduction in the overall $\chi^{(3)}$, a frequency dependence study of $\chi^{(3)}$ is currently being investigated.

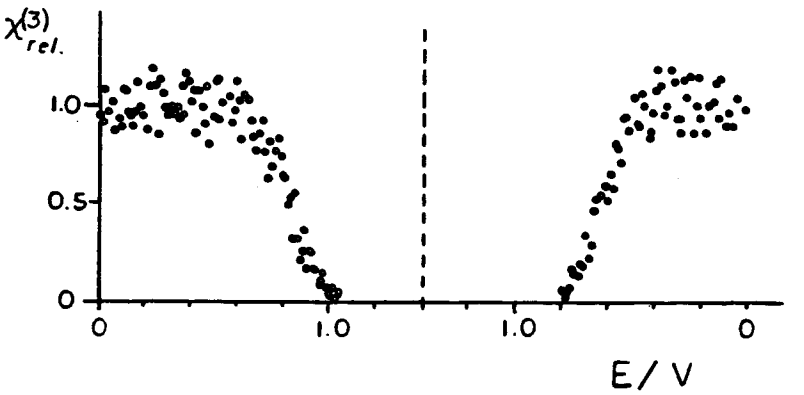

FIGURE 6 Change in the relative value of $\chi^{(3)}$ in the course of redox cycle of the electrochemically prepared polythiophene. A triangular voltage sweep had the highest value at +1.4V, the position of which is indicated by the vertical dashed line.

CONCLUSIONS

In polymers, where the photoexcitation generates charge carriers, we have investigated the resonant $\chi^{(3)}$ behavior. The observed resonant $\chi^{(3)}$ value and its time response vary over a wide range. The resonant values, however, do not achieve sufficient enhancement to compare favorably with what is obtainable for resonant nonlinearities in multiple quantum-well inorganic semiconductors.

Acknowledgment

This research was supported in part by the Air Force Office of Scientific Research under contract number F4962087COO42 and in part by NSF Solid State Chemistry program under grant number DMR 8403987.

References

1. Y. R. Shen, "The Principles of Nonlinear Optics" Academic Press, Inc. (New York, 1984).
2. R. A. Fisher, "Optical Phase Conjugation" Academic Press, Inc. (New York, 1983).
3. E. J. Eichler, P. Günter and D. W. Pohl, "Laser-Induced Dynamic Gratings" Springer-Verlag (Berlin, Heidelberg, 1986).
4. "Nonlinear Optical Properties of Organic and Polymeric Materials" Ed. D. J. Williams, Am. Chem. Soc. Pub. (Washington D.C., 1983).
5. "Nonlinear Optical Properties of Organic Molecules and Crystals" Vols 1 and 2, Eds. D. S. Chemla and J. Zyes, Academic Press, Inc. (Orlando, Florida, 1987).
6. "Nonlinear Optical and Electroactive Polymers" Eds. P. N. Prasad and D. R. Ulrich (Plenum Press, New York, 1988).
7. D. S. Chemla in "Nonlinear Optics: Materials and Devices" Ed. C. Flytzanis and J. L. Ouder, Springer-Verlag, Berlin (1986) p. 65.
8. "Handbook of Conducting Polymers" Volumes 1 and 2, Ed. T. Skotheim (Marcel Dekker, New York, 1986).
9. G. B. Blanchet, C. R. Fincher, T.-C. Chung and A. J. Heeger, *Phys. Rev. Lett.*, **50**, 1938 (1983).
10. D. N. Rao, P. Chopra, J. Swiatkiewicz, S. K. Ghoshal and P. N. Prasad, *J. Chem. Phys.*, **84**, 7049 (1986).
11. D. N. Rao, J. Swiatkiewicz, P. Chopra, S. K. Ghoshal and P. N. Prasad, *Appl. Phys. Lett.*, **48**, 1187 (1986).
12. T. M. Ding and E. Garmire, *Appl. Opt.*, **22**, 3177 (1983).
13. I. Kminek and J. Trekoval, *Makromol. Chem. Rapid Commun.*, **5**, 53 (1984).
14. M. A. Druy and R. J. Seymour, *J. de Phys. Coll.*, **44**, C3-595 (1983).
15. J. M. Pearson and M. Stolka, "Poly(*N*-vinyl) Carbazole" edited by M. B. Hughlin, Gordon and Research Scientific Publisher, New York (1981).
16. A. J. Heeger, D. Moses and M. Sinclair, *Synthetic Metals*, **17**, 343 (1987).
17. F. Kajzar, S. Etemad, C. L. Baker and J. Messier, *Synthetic Metals*, **17**, 563 (1987).
18. W. P. Su and J. R. Schreffer, *Proc. Nat. Acad. Sci. USA*, **77**, 5626 (1980).

19. C. V. Shank, R. Yen, R. L. Fock, J. Orenstein and G. L. Baker, *Phys. Rev. Lett.*, **49**, 1660 (1982).
20. Z. Vardeny, J. Strait, D. Moses, T. C. Chung and A. J. Heeger, *Phys. Rev. Lett.*, **49**, 1657 (1982).
21. Z. Vardeny, E. Ehrenfreund, O. Brafman, M. Nowak, H. Schaffer, A. J. Heeger and F. Wudl, *Phys. Rev. Lett.*, **56**, 671 (1986).
22. K. Kanets, Y. Kohno and K. Yoshino, *Solid State Commun.*, **51**, 267 (1984).
23. K. Kanets, Y. Kohno and K. Yoshino, *Mol. Cryst. Liq. Cryst.*, **118**, 213 (1985).
24. C. P. deMelo and R. Silbey, *Chem. Phys. Lett.*, (in press).